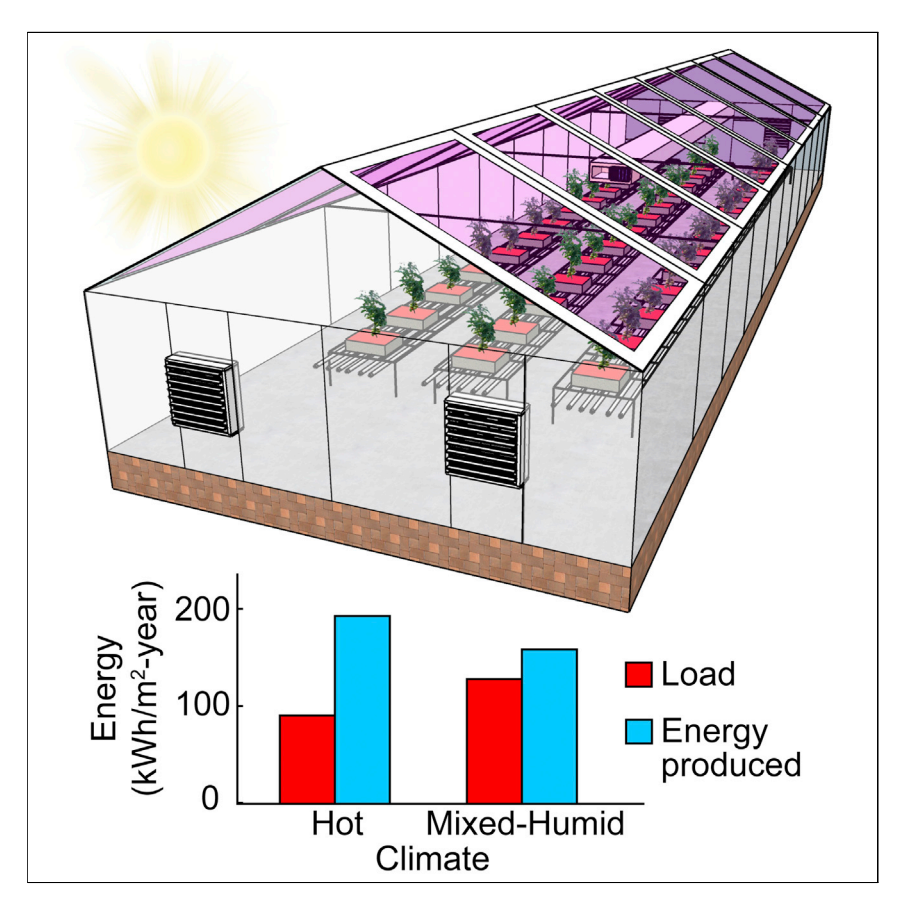
Joule Cell^Press

Article

Achieving Net Zero Energy Greenhouses by Integrating Semitransparent Organic Solar Cells



A dynamic energy model is used to demonstrate that semitransparent organic solar cells (OSCs) can be employed on greenhouses to achieve net zero energy greenhouses in warm and moderate climates. Furthermore, it is shown that the reduction in sunlight entering the greenhouses is not as significant as the transmittance of the OSCs would suggest owing in part to the OSCs replacing the need for shade-cloths. These results demonstrate the significant opportunity of OSC-greenhouses for high-yield, environmentally friendly agriculture.

Eshwar Ravishankar, Ronald E. Booth, Carole Saravitz, Heike Sederoff, Harald W. Ade, Brendan T. O'Connor

btoconno@ncsu.edu

HIGHLIGHTS

Introduce detailed energy balance model for OSC integrated greenhouses

Reveal that net-zero energy greenhouses can be realized with OSC integration

Show that low-e nature of the OSC can lead to energy savings throughout the year

OSCs are found to effectively replace shade cloths minimizing sunlight attenuation

Ravishankar et al., Joule 4, 1–17 February 19, 2020 © 2019 Elsevier Inc. https://doi.org/10.1016/j.joule.2019.12.018

CellPress

Article

Achieving Net Zero Energy Greenhouses by Integrating Semitransparent Organic Solar Cells

Eshwar Ravishankar,¹ Ronald E. Booth,¹ Carole Saravitz,² Heike Sederoff,² Harald W. Ade,³ and Brendan T. O'Connor^{1,4,*}

SUMMARY

Greenhouses vastly increase agricultural land-use efficiency. However, they also consume significantly more energy than conventional farming due in part to conditioning the greenhouse space. One way to mitigate the increase in energy consumption is to integrate solar modules onto the greenhouse structure. Semitransparent organic solar cells (OSCs) are particularly attractive given that their spectral absorption can be tuned to minimize the attenuation of sunlight over the plants photosynthetically active spectrum. Here, the benefits of integrating OSCs on the net energy demand of greenhouses within the U.S. are determined through a detailed energy balance model. We find that these systems can have an annual surplus of energy in warm and moderate climates. Furthermore, we show that sunlight reduction entering the greenhouse can be minimized with appropriate design. These results demonstrate that OSCs are an excellent candidate for implementing in greenhouses and provide an opportunity to diversify sustainable energy generation technology.

INTRODUCTION

The combination of global warming, a growing global population, and the increasing scarcity of fresh water are expected to put significant stress on conventional agriculture.^{1,2} One approach to relieve this impending crisis is greenhouse based agriculture, which reduces water consumption while greatly increasing annual crop production by creating a suitable environment for plants to grow irrespective of outdoor environment.3 However, greenhouse operation comes with its own set of challenges. While the desired plant environment can be maintained by heating and cooling the space, this results in a significant increase in energy consumption relative to conventional farming. This energy input can constitute the highest percentage of a greenhouse's environmental impact.⁴ For greenhouses to become a viable solution for sustainable agriculture, a means to offset the large energy consumption is needed, ideally with minimal environmental impact. At the same time, solar power has made considerable progress in terms of utility scale adoption,⁵ as well as advancements in thin film technologies that include organic solar cells (OSCs).6,7 These agricultural needs and technology developments have led to recent interest in integrating solar power with greenhouses.^{8,9}

Approaches to integrate solar power with greenhouses can be categorized as (1) adjacent, (2) shared structure, and (3) shared structure and sunlight systems. Given that land use efficiency is becoming increasingly important environmentally, along with a desire for co-locating agriculture and population centers, strategies that share

Context & Scale

Current agricultural practices are putting enormous stresses on the environment that includes unsustainable water usage, deforestation, and pesticide runoff. These stresses are expected to get more severe in the coming years due to the need to feed an increasing global population. One promising approach to reduce environmental impact is greenhouse-based agriculture that can significantly increase land use efficiency while reducing water consumption and pesticides. However, a major limitation of greenhouses is the significantly higher energy consumption used to condition the space. Here, we show that semitransparent organic solar cells (OSCs) can enable net zero energy (NZE) greenhouses and thus provide a significant opportunity to advance environmentally sustainable agriculture. Furthermore, we show that the unique attributes of organic solar cells are well suited for synergistic greenhouse integration providing a potential route for broad commercial adoption of OSCs.



the same land are preferred. By sharing the structure, there are also potential economic advantages, including balance of system savings associated with using the greenhouse structure to support the solar modules. 10 One approach in sharing the structure is employing opaque solar modules on the greenhouse roof. 11-14 However, these solar modules compete with the plants for sunlight resulting in crop yield loss, which has limited broad adoption. 9,14 To overcome this weakness, strategies where sunlight over the photosynthetically active radiation (PAR) spectrum (400-700 nm) continues to reach the plants while also using portions of the sunlight for power generation are desired. These include the use of wavelength-selective optics to direct sunlight toward opaque photovoltaic modules, 15 luminescent solar concentrators, 16 and the use of semitransparent wavelength-selective photovoltaics.¹⁷ Wavelength-selective focusing lenses face several challenges including: focusing primarily direct sunlight, requiring solar tracking, and complex greenhouse structures that can be cost prohibitive. 15,18 Luminescent solar concentrators provide a simpler system but to date suffer from low power conversion efficiency. 16 A promising alternative is to use semitransparent photovoltaics. In this case, organic solar cells (OSCs) are particularly attractive given that the active layer absorption spectrum can be readily tuned through material selection, the devices are amenable to low cost production methods, and the devices are thin and light weight enabling simple integration onto a greenhouse structure. 19-22

The promise of OSCs is justified due to recent rapid advancements in non-fullerene small molecule electron acceptors that have led to significant increases in OSC power conversion efficiency, with many reports of 14%-16% devices bringing the technology closer to commercial relevance. 22-25 Yet, the cost of silicon based solar power continues to drop making alternative solar energy technologies difficult to penetrate the market.⁵ To achieve widespread adoption, OSCs must find applications that take advantage of its unique properties. Organic solar powered greenhouses are one such potential avenue. For this to occur, OSC-greenhouses will need favorable economics, minimal impact on crop yield, and have an ability to provide a significant portion of the energy demand of the greenhouse. A feasibility analysis performed by Emmott et al. in 2015 revealed that high efficiency OSCs coupled with high transmittance electrodes have the potential to result in cost effective OSCgreenhouses.¹⁷ As OSC efficiencies continue to improve so does the economic outlook of employing them in greenhouses. 10 In addition, there have been studies showing that semitransparent solar cells, 26 and LSCs27 can be employed in greenhouses and achieve similar plant growth. While further research is needed to establish the full impact of solar cell integration on agriculture yield, these initial studies show promise that sharing sunlight approaches can be effective. What has not been considered to date, and is sorely needed, is the potential for OSCs to significantly improve the energy outlook of greenhouse-based agriculture. Through detailed energy balance analysis, the environmental impact of OSC-greenhouses can be established providing a clear view of the opportunity to achieve more sustainable agriculture practices.

In this report, we introduce a tailored energy balance model for OSC-greenhouses to gain an improved understanding of the potential of such systems to meet the energy needs of greenhouses. This includes not only the solar power generated but how the greenhouse energy load changes when the OSC modules are employed. We consider two semitransparent OSC systems that are known to have high performance and varying spectral absorption characteristics. A key factor impacting greenhouse energy demand is its geographical location and thus three distinct locations are considered across the United States: Phoenix, AZ, Raleigh, NC, and Antigo,

¹Department of Mechanical and Aerospace Engineering, North Carolina State University, Raleigh, NC 27695, USA

²Department of Plant and Microbial Biology, North Carolina State University, Raleigh, NC 27607, USA

³Department of Physics, North Carolina State University, Raleigh, NC 27695, USA

⁴¹ and Contact

^{*}Correspondence: btoconno@ncsu.edu https://doi.org/10.1016/j.joule.2019.12.018



WI. These locations are chosen as they represent regions that have a substantial greenhouse agriculture market,³ and represent three characteristic climate zones described by the US Department of Energy as hot-dry, mixed-humid, and cold, respectively.²⁹ Below we first provide an overview of the greenhouse and the computational model used to determine the energy balance of the system. As part of this discussion, we consider the importance of managing infrared (IR) light through solar cell design, and the modified use of shade cloths. We then show the expected changes in radiation entering the greenhouse when employing the semitransparent OSCs. It is found that the drop in radiation due to the roof mounted OSCs is partly mitigated in the winter by the lower solar altitude angle resulting in a large fraction of light entering through the greenhouse wall, and during the summer by removing the need for shade cloth deployment to manage the greenhouse temperature. While there is a drop in solar radiation entering the greenhouse in the winter, when adding the OSCs, the OSC-greenhouses incur a lower heating demand than the conventional greenhouse. This is attributed to low emissivity (low-e) characteristics of the OSC stack, providing an added benefit to the power generation. Through this analysis it is shown that the OSC-power generation can meet the thermal energy demands of a greenhouse in warm and moderate climates. In the cold climate the OSCs cannot meet the annual energy demands of the greenhouse but continue to provide a substantial fraction of its energy needs. Finally, we extend the analysis to consider a conceptual solar cell active layer that has an approximate 400 nm absorption bandwidth and an absorption edge that is selected freely. This simple first order model demonstrates that an OSC with active layers that absorb in the near IR with minimal impact on transmittance over the PAR spectrum will continue to meet the energy needs of a greenhouse in hot and moderate climates. In summary, this research shows that semitransparent OSCs are well suited to meet the thermal energy demands of a greenhouse, and with further spectral tuning may compliment the plant needs for effective low-energy, high productivity-controlled environment agricultural systems.

Model

Greenhouse Energy Balance

Approaches to model the microclimate in a greenhouse have been well documented by Sethi et al.³⁰ Models range from simple static models to size the heating and ventilation systems³¹ to dynamic models that make use of mass and energy balances to model various systems in the greenhouse environment. Dynamic models are typically preferred over static models because of improved precision in predicting the energy demand (\pm 10% error) as well as the interior climate of the greenhouse. ^{32–35} There are commercial software packages (e.g., ESP-r and Energy Plus) that can dynamically model greenhouse environments.³⁶ However, these programs are incapable of integrating semitransparent solar cells, particularly with unique spectral characteristics. In addition, by developing a custom model, the spectral information along with the local plant environment (temperature, humidity, etc.) are captured for potential future studies on plant growth. 36 Considering these needs, we introduce a detailed dynamic energy balance model to compute the hourly heating and cooling demand of a conventional and OSC-greenhouse. Below, major features of the model are described with a more complete description provided in the Supplemental Information.

Heating and cooling demand for the greenhouse was calculated based on the energy flux between the greenhouse and its environment. These fluxes are formulated based on known ambient conditions, solar insolation, and physical elements of the greenhouse.^{34,37} The components of the greenhouse considered are broadly

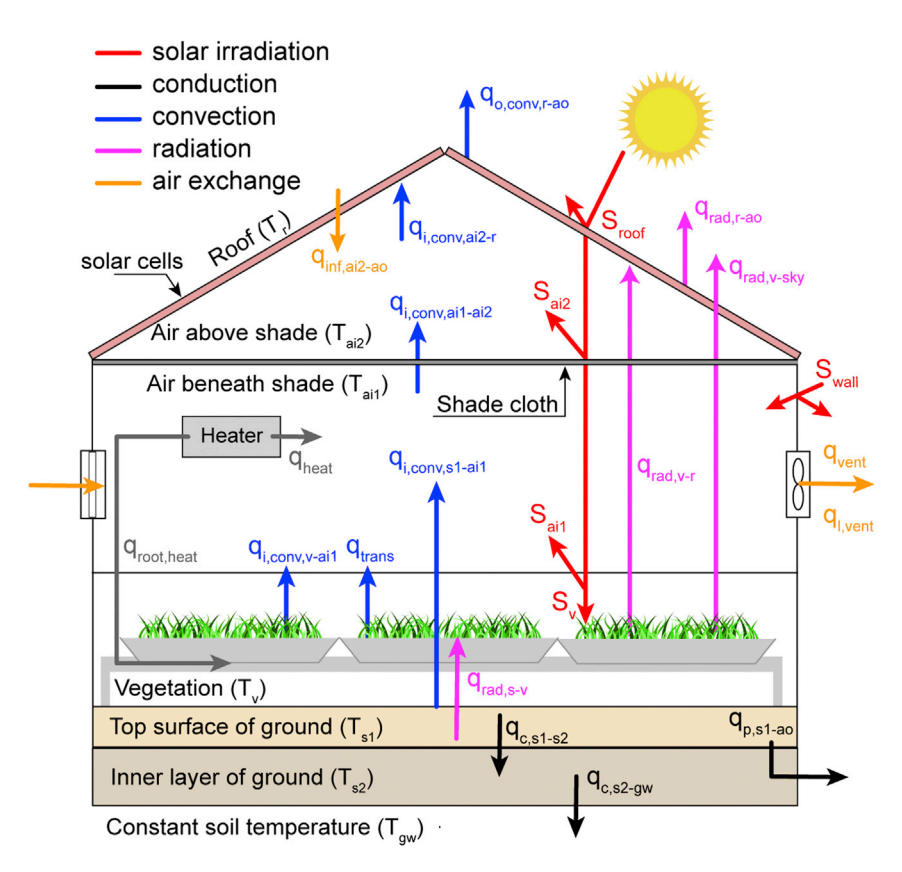


Figure 1. Schematic of the Energy Fluxes for OSC-Greenhouse with Shades Deployed
The energy balance terms are defined in the Supplemental Information and include the
temperature of the various elements (T), the absorbed solar radiation (S), and sensible and latent
heat transfer terms (q).

divided into the inner layer of soil, surface soil layer, vegetation layer, air inside the greenhouse, and roof. 34,37 The energy fluxes associated with each component for the OSC-greenhouse with shades deployed are provided in Figure 1, whereas the case without shades is provided in Figure S1. Parameters used for the greenhouse energy model are given in Table S1. The outdoor temperature and humidity conditions for each location were taken hourly from typical meteorological year 3 (TMY3) data set.³⁸ To visualize the different climate for each location, the average monthly ambient temperature and relative humidity for each location is given in Figure S2. The latent load of the greenhouse due to transpiration from plants and air exchange due to infiltration and ventilation were computed based on the correlations suggested by Joliet et al.³⁹ The energy demand for heating does not account for heating system efficiency, while the energy demand for cooling is based on the on electricity used to operate an evaporative fan and pad cooling system. The accuracy of the model was verified by validating it with existing experimental data and models found in the literature, 31,40,41 which is discussed further in the Supplemental Information. All simulations were conducted in MATLAB executed on a high-performance computing system cluster.

The primary aim of this model is to assess energy balance of an OSC integrated greenhouse across a variety of crops. In the model, crop yield is not considered directly given the complex dependence of plant growth on the quality and quantity of radiation. ⁴² While we do not explicitly consider the impact of the modified lighting

CellPress

on plant growth, we report changes in PAR radiation in the greenhouse as an indirect view of potential crop impact. However, it is important to acknowledge that in addition to absorption over the PAR spectrum by chlorophyll, plants also have photoreceptors that include carotenoids that absorb in the UV (320-400 nm) and phytochromes that absorb in the far red (650-730 nm).⁴² Pollinators also use UV light. The impact of radiation over these wavelengths would also need to be considered in future plant growth studies. While the analysis does not consider crop yield, we establish indoor temperature set points based on tomatoes, which were 21°C-28°C during the day and 17°C-18°C during the night. 40,43 This also dictates the greenhouse relative humidity set point of 60%-80%. 40,43 Tomatoes are chosen here as a guide, since they represent one of the largest greenhouse crops globally. 44 This includes commercial greenhouses in similar climates to the locations chosen for analysis. For example, Arizona has one of the largest greenhouse tomato firms in the country.³ North Carolina ranks among the top ten greenhouse tomato producing states in the country, and Antigo, WI due to its latitude has a climate similar to southern Canada where nearly 40% of US tomato demand is met.³

Description of the Greenhouse

A 29.4 × 7.3 m single span gable-roof greenhouse with a gutter height of 3 m was analyzed, which is representative of a standard commercial greenhouse.⁴⁵ The greenhouse is schematically shown in Figure 2A. It is oriented north-south, which is typical as it reduces structural shadows being locked into a specific location of the greenhouse. In current design practice, a roof slope of 27°-30° is typically chosen, 46 and here we consider the roof to have a tilt angle of 27° independent of location. The roof and walls excluding the north facing wall were made up of 4 mm thick single pane glass. The north wall was considered an adiabatic surface, as it often interfaces with a building used for storage or offices (i.e., head house). The greenhouses under consideration were assumed to operate year around. Mechanical ventilation was provided by two 1.5 hp fans that are located on the walls of the greenhouse. 47 The fans are considered to have two-speeds with the low speed capable of supplying 2 air changes per hour (ACH) and the high speed setting providing 60 ACH. 46 Infiltration was set at 1 ACH and indoor air velocity was assumed to be 0.15 m/s. 46 To provide further cooling evaporative pads were employed. 48 Heating was supplied by a forced hot air furnace and radiant root heating system. The radiant heating was used to provide high efficiency thermal management of the plants but has a limited heat flux to avoid plant stress. One design feature of note is that in the conventional greenhouse shade cloths are employed during the daytime in the summer to reduce heat gain and during the night in the winter to reduce heat loss. 49 In this analysis, shades are deployed at night during the winter for both the conventional and OSC-greenhouse. In the summer months, the conventional greenhouses deploy shades during the day as needed to manage the temperature in the greenhouse but are not deployed in the OSC-greenhouse given the already reduced transmittance from the OSCs. Details of the shade deployment schedule is given in Table S1. A commonly used shade cloth with 50% transmittance was used here and placed at gutter height as illustrated in Figure 1.50 When the shade was deployed it is assumed to cover all light entering through the roof while light entering through the walls of the greenhouse remains unshaded. While whitewash paint can be applied to the walls for additional summer shading,⁵¹ it was not considered here.

Solar Power and Light Entering the Greenhouse

Accurately describing the incident solar insolation onto the greenhouse surface is critical to modelling the thermal load of the greenhouse as well as the energy



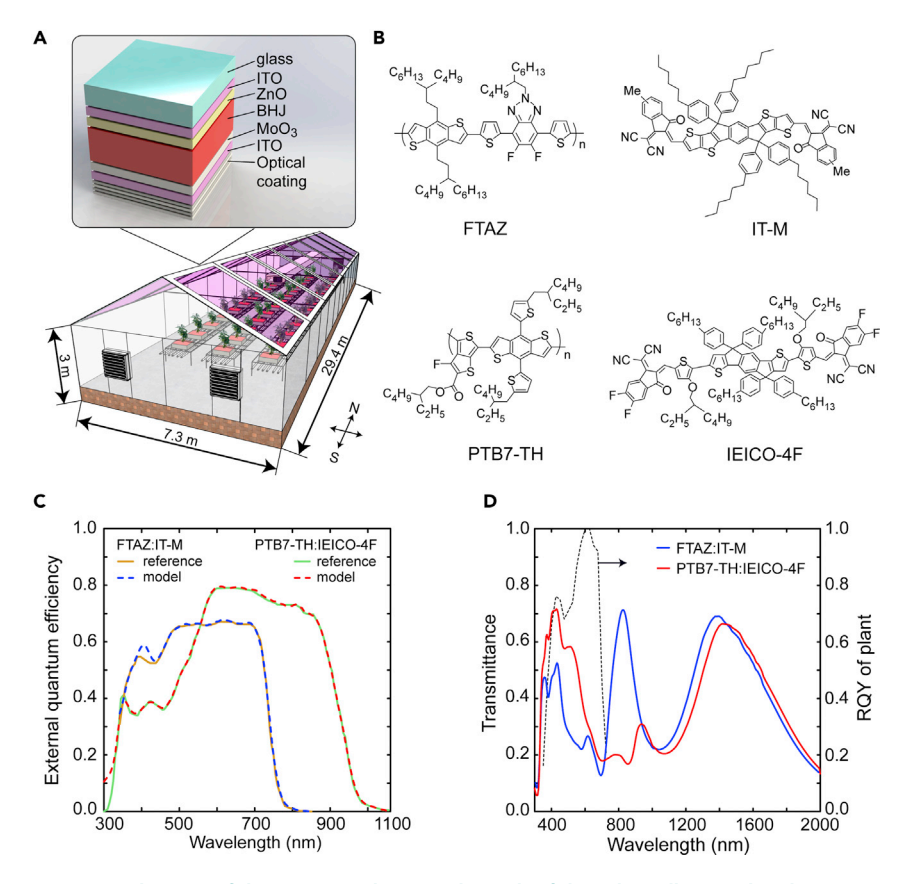


Figure 2. Schematic of the OSC-Greenhouse and Details of the Solar Cells Considered

- (A) Depiction of the greenhouse and OSC stack with the dielectric Bragg reflector.
- (B) Molecular structure of the polymers used in the solar cell active layer.
- (C) Comparison of the modelled external quantum efficiency to experimental results adapted from previous reports. 25,28
- (D) Transmittance of modelled OSCs and relative quantum yield (RQY) of vegetation. 52

production by the solar cells. Here, the daily integration (DI) method was used to determine the beam (direct), diffuse, and ground reflected radiation incident on the walls and roof of the greenhouse. ^{53,54} Effective incident angles for diffuse and reflected solar radiation incident on the surface of the greenhouse was computed assuming isotropic light scattering conditions. ⁵⁵ Inputs of this model include the terrestrial monthly average, daily total, and diffuse radiation on a horizontal surface, which was obtained for each location from NASA-SSE. ⁵⁶ From the incident radiation, the transmittance of light into the greenhouse and the absorption of light by the solar cells was determined by employing a transfer matrix model. ^{57,58} See Supplemental Information for additional details.

To understand the impact of the OSC spectral characteristics on energy load, two OSCs which differ only in the active layer were considered. The two active layers were a blend of FTAZ and IT-M, and a blend of PTB7-TH and IEICO-4F, with their molecular structure provided in Figure 2B. These active layers were considered as they have both been demonstrated with similar high efficiencies of 11% and 12% in opaque devices, ^{25,28} and have unique spectral absorption characteristics. PTB7-TH:IEICO-4F was selected due to the absorption being weighted strongly in the near IR, which minimizes the drop in transmittance in the PAR spectrum. ^{25,59} This active layer has also been used to demonstrate successful mung bean growth under



semitransparent OSCs.²⁶ The FTAZ:IT-M has a similar efficiency but with greater absorption over the PAR spectrum. Considering these active layers allows for a view of how the change in absorption profile impacts heating and cooling loads and radiation over PAR entering the greenhouse. The solar cell structure is illustrated in Figure 2A and consists of a 100 nm thick indium tin oxide (ITO) layer used for the front electrode followed by a 35 nm thick ZnO electron transport layer, then the active layer. The active layer thickness was initially set to values reported to optimize opaque solar cell performance and were 105 nm for FTAZ:ITM and 126 nm for PTB7-TH:IEICO-4F.^{25,28} After the active layer there is a 5 nm MoO₃ layer hole transport layer followed by another 100 nm thick ITO electrode. This solar cell structure is then sandwiched between 2 mm thick layers of glass. One layer of glass also acts as the surface of the greenhouse. The use of glass also provides reliable encapsulation with extremely low permeability to oxygen and water maximizing device lifetime. 60 The optical constants used in the model of the OSCs are given in Figures S3A and S3B. ITO inherently has a high IR reflectivity and acts as an effective low-emissivity (low-e) coating. 61 To further improve IR reflection as a way to manage thermal load of the greenhouse and to maximize transmittance over PAR a 4-layer dielectric stack was employed after the back ITO electrode. 62 This consists of alternating LiF and MoO_3 layers with thickness optimized based on maximizing transmittance of the OSC from 400-700 nm and maximizing reflectance from 900-2,000 nm. The coating was limited to 4-layers to maintain cost-effective solar cells. The thickness for the dielectric stack (LiF/MoO3/LiF/MoO3) optimized for FTAZ:IT-M and PTB7-TH:IEICO-4F are 180 nm/90 nm/150 nm/110 nm, and 180 nm/90 nm/ 170 nm/100 nm, respectively. The thickness of the layers was obtained by simulating all possible combinations from 1-200 nm layer thickness in 1 nm increments. Given the large number of permutations, the program was run in parallel on a high-performance computer cluster. The resulting transmittance of the solar cells are given in Figure 2D showing the wavelength averaged transmittance over PAR of 32% and 45% for the FTAZ:IT-M and PTB7-TH:IEICO-4F solar cells, respectively. The transmittance averaged over the short wavelength IR (1,000-2,000 nm) is 43% and 36%. The Bragg reflectors results in a 17% drop in short-wave IR transmittance for both FTAZ:IT-M and PTB7-TH:IEICO-4F solar cells, illustrating the utility of the coatings. In addition, the dielectric stack leads to an increase in power conversion efficiency (PCE) of 5% and 10% for the FTAZ:IT-M and PTB7-TH:IEICO-4F based OSCs, respectively. Finally, for simplicity, we do not consider bus lines or module framing but rather assume the active solar cell area covers 85% of the roof area.

To estimate the power produced by the OSCs we first use the optical modelling to predict the photocurrent. The absorption in the active organic semiconductor layer was first determined by transfer matrix modeling. From the light absorption and internal quantum efficiency (IQE) the external quantum efficiency (EQE) was determined. The EQE of opaque OSCs from previous experimental reports were compared to the model with results given in Figure 2C, showing good agreement. Here the IQE was estimated based on reports of high performance OSCs, 25 and then adjusted slightly to improve the EQE model fit. The estimated IQE of the OSCs is given in Figure S3C and was used throughout the modeling of the semitransparent OSCs. From the EQE and incident radiation the short circuit current (J_{SC}) of the OSCs were determined. The modelled J_{SC} was found to match the previous reported experimental results well.^{25,28} The power produced from the solar cells was then calculated assuming approximate values for the OSC open circuit voltage (V_{oc}) and fill factor (FF) using experimental results for realistic estimates. ¹⁷ The V_{OC} of FTAZ:ITM and PTB7-TH:IEICO-4F were taken as 0.95 and 0.72 V under 1-sun illumination, respectively. The V_{oc} was then varied depending on the photocurrent using a



photodiode equation.⁶³ A FF of 0.7 was assumed for both OSCs based on experimental results.¹⁷ The modelled efficiency for opaque devices (i.e., with a Ag reflective back electrode) under AM 1.5G conditions (1,000 W/m²) was approximately 11% and 12%, matching what has been found in the literature for similar device structures.^{25,28} The modelled efficiency for the semitransparent OSCs was approximately 9.5% and 10%, respectively. Note that a temperature dependence of the OSC performance was not considered. Finally, a derating factor is an important parameter when considering system performance, to account for losses associated with inverters, connections, and soiling. A derating of up to 15% is often assumed, which depends on a range of factors of the system design and grid connection.⁶⁴ Here, we do not directly apply a derating factor but consider OSCs that have efficiencies considerably lower than the best reported cells of over 16%,²³ resulting in a conservative estimate of power produced.

RESULTS

The results of the modelling for the three diverse climates are reviewed in this section. The results show that the energy balance between the two solar cells are similar and thus a focus is placed on the PTB7-TH:IEICO-4F based solar cells given its greater transmittance over PAR. Comparative FTAZ:IT-M based solar cell results are primarily given in the Supplemental Information.

Heating and Cooling Load

The monthly heating load for both the conventional and PTB7-TH:IEICO-4F OSCgreenhouse is shown in Figure 3 (with FTAZ:IT-M given in Figure S4). It is found that in all three locations, the OSC-greenhouses have a decrease in the heating load compared to the conventional greenhouse due to the low-e nature of the solar cells resulting in lower thermal radiation losses. This decrease is highest in AZ where the heating load dropped by 54%, followed by NC (46% drop) and then WI (32% drop). The cooling load is met by fans used for ventilation and evaporative cooling. The monthly energy consumption by the fans is given in Figure 3 for both the conventional and OSC-greenhouse. The energy consumption by the fans is also reduced in the OSC-integrated greenhouses compared with the conventional greenhouse in all three climate locations. This decrease is the greatest in WI where the cooling load dropped by 12%, followed by NC (8% drop), and then AZ (6% drop). This reduction in cooling load is due in part to the drop in solar insolation entering the OSC-greenhouses due to the semitransparency of the solar cells. This includes light absorbed by the solar cell as well as the low-e nature of the OSCs that assists in reducing the thermal gains from the IR portion of sunlight.

The impact of OSC integration on the water consumption used by the evaporative pad cooling system is shown in Figure S5. The reduction in cooling load in the OSC-greenhouse in AZ results in lower water consumption compared to the conventional greenhouse. However, in both NC and WI water consumption by fan and pad cooling system in the OSC-greenhouse is comparable to the conventional greenhouse. In AZ, the OSCs continually provide shading throughout the year lowering the solar gain in the greenhouse and thus reducing evaporative cooling demand. In NC and WI, the evaporative cooling demand is timed more closely with the use of the shade cloths in the conventional greenhouse. As discussed below, the OSC-greenhouse and conventional greenhouse with shades deployed have similar radiation enter the greenhouse and therefore these systems have similar water consumption associated with evaporative cooling.

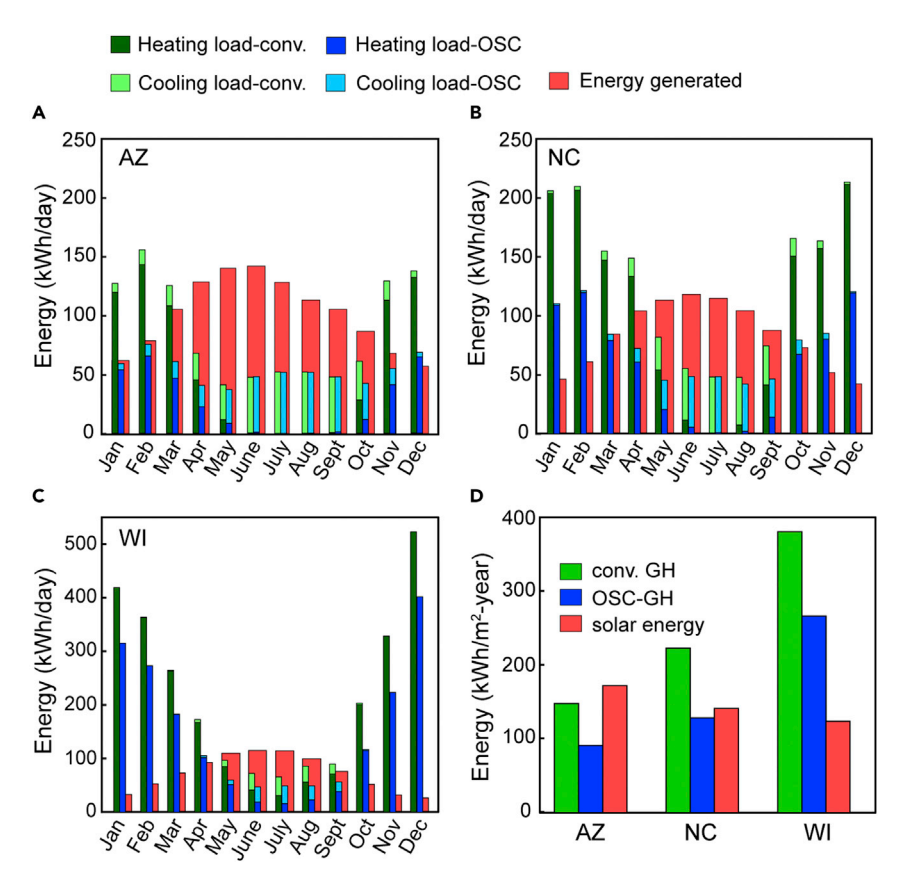


Figure 3. Monthly Average Energy Demand and Generation for Conventional and PTB7-TH:IEICO-4F OSC Integrated Greenhouse

- (A) Heating demand, ventilation energy demand, and energy generation in Arizona (AZ).
- (B) Heating demand, ventilation energy demand, and energy generation in North Carolina (NC).
- (C) Heating demand, ventilation energy demand, and energy generation in Wisconsin (WI).
- (D) Annual total energy demand and energy generation for AZ, NC, and WI.

Meeting the Load with Solar Power

The energy harnessed by the OSCs is given on a monthly basis and annually in Figure 3A–3D. As expected, the power generation by the OSCs is largest in the summer and drops in the winter months. In AZ there is a surplus of energy production for the entire year, with every month producing surplus power. This results in the solar cells producing nearly 2 times more energy than necessary to meet the heating and cooling load. In both NC and WI, the solar cells continue to produce a surplus of energy in the summer but are unable to meet the monthly demand in portions of the winter months. On an annual basis, we find that in NC the solar cells exceed greenhouse energy demand producing 10% more energy than needed, while in WI the solar cells meet 46% of the total greenhouse energy demand.

DISCUSSION

Differences in Plant Irradiation

At this stage it is important to highlight that the reduction in radiation into the OSC-greenhouse is not as large as the transmittance of the organic solar cells would suggest as shown in Figure 4 for PTB7-TH:IEICO-4F OSCs and in Figure S6 for FTA-Z:IT-M OSCs. While the PTB7-TH:IEICO-4F OSCs has a transmittance of 36% over the entire solar spectrum, the total light transmitted into the OSC-greenhouse is

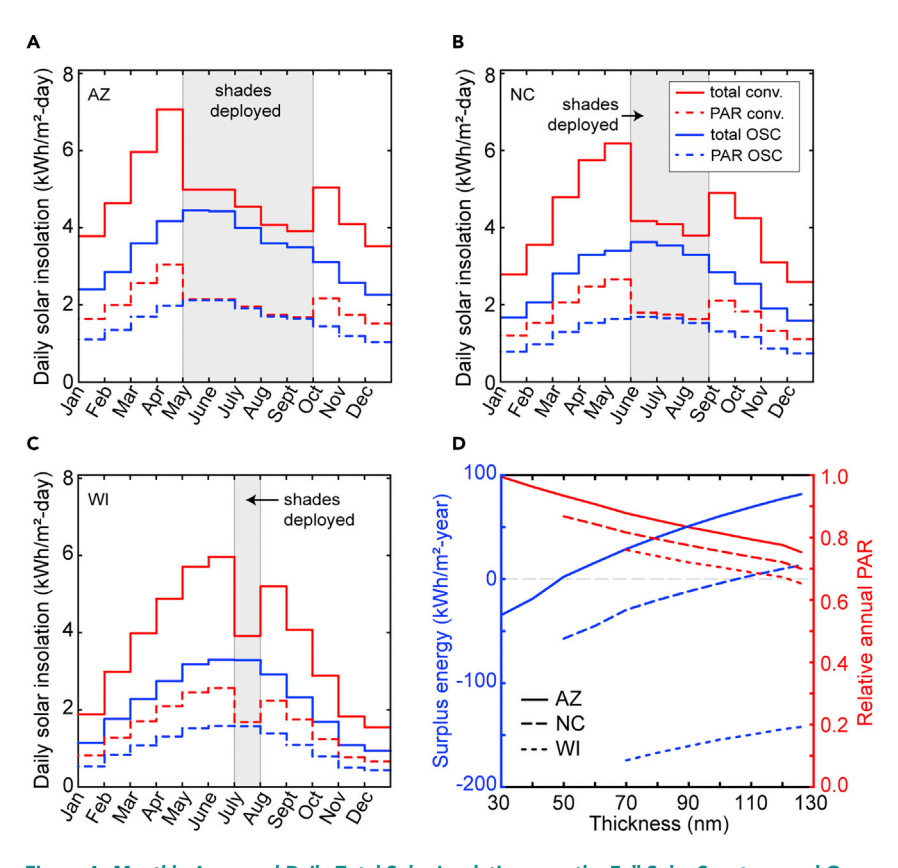


Figure 4. Monthly Averaged Daily Total Solar Insolation over the Full Solar Spectrum and Over PAR Incident on Plants for Conventional (Conv.) and PTB7-TH:IEICO-4F OSC-Greenhouses

- (A) Arizona (AZ)
- (B) North Carolina (NC).
- (C) Wisconsin (WI).
- (D) Annual energy balance and relative drop in annual insolation over PAR for PTB7-TH:IEICO-4F OSC-greenhouses with variation in active layer thickness for AZ, NC, and WI.

only 32% lower than the conventional greenhouse in AZ in January. This difference is due to the sun's path over the course of the day and season (i.e., day arc). In the morning and evening a significant fraction of sunlight enters the greenhouse through the walls. In addition, during the winter the sun has a lower altitude angle resulting in a further increase in sunlight entering the through the greenhouse walls. This radiation is not captured by the solar cells and enters the greenhouse space in the same manner as the conventional greenhouse. This pattern is seen in all three locations with a progressively greater fraction of light entering through the walls of the greenhouse as the greenhouses move north in latitude. Furthermore, in the summer months, the conventional greenhouse deploys shades with 50% transmittance during the day following the schedule given in Table S1 to reduce greenhouse overheating. As shown in Figure 4, in months where the shades are deployed, the total irradiation incident on the plants is approximately 10% lower in the OSC-greenhouse compared to the conventional greenhouse in AZ. However, the irradiation over the PAR spectrum during these months is comparable for both the OSC and conventional greenhouse. These results have important implications for not only energy load but also plant growth. While plant growth is not directly considered in this study, the results show the expected changes in the light transmitted over the PAR spectrum between the conventional and OSC-integrated greenhouses, from which impact on plant growth may be inferred.



To this point the analysis has been for active layer thicknesses that lead to the best performance OSCs for opaque devices, but this may not be the optimal case for integrating semitransparent devices on greenhouses. To assess this, we considered the impact of varying the active layer thickness on the energy produced and impact on radiation over the PAR spectrum entering the greenhouse. The electrodes of the OSC stack remain the same and at each active layer thickness the dielectric layer is re-optimized. The active layers thickness from 30 nm to 130 nm was considered. The annual energy balance results for the two active layers and for all three locations are given in Figures 4D and S7. Also plotted is the relative drop in the annual radiation over the PAR spectrum entering the greenhouse with the addition of the OSCs. In AZ, OSCs with active layer as thin as 50 nm still generates surplus energy. For the PTB7-TH:IEICO-4F active layer, this results a reduction in annual radiation over the PAR spectrum of approximately 10% relative to the conventional greenhouse. In NC, Net Zero Energy (NZE) is achieved at an active layer thickness of approximately 110 nm for both FTAZ:IT-M and PTB7-TH:IEICO-4F integrated greenhouse, which is close to the optimal thickness found for opaque devices. ^{25,28} At this thickness, the PTB7-TH:IEICO-4F integrated greenhouse had a 25% reduction in annual radiation over the PAR spectrum.

Hourly Energy Balance

Insights into the energy balance can be gained by looking at the hourly energy load and the greenhouse interior temperature. The most illustrative cases are characteristic days in the winter and summer taken here as January 7th and July 26th for AZ. The days of the month which best represent the average monthly outdoor ambient temperature and relative humidity were selected. The comparison of the conventional greenhouse and the PTB7-TH:IEICO-4F OSC-greenhouse for AZ is given in Figure 5, and the cases for NC and WI is given in Figures S8 and S9.

First considering January, we see that in AZ heating is needed at night, but during the day the solar gains are significant enough that ventilation to cool the greenhouse is still necessary. It is shown that the heating requirement is lower at night in the OSC-integrated greenhouse due primarily to the low-e OSC. During the day the ventilation energy load of the OSC-greenhouse was also reduced given the lower radiation entering the greenhouse. Similarly, in the cold climate (WI), the low-e OSC reduces heat loss in the greenhouse at night. During the day, the OSC greenhouse has lower transmittance resulting in a lower interior greenhouse temperature. However, the greenhouse air's moisture content remains similar with respect to a conventional greenhouse, and thus the lower temperature raises the relative humidity of greenhouse. This leads to a need for more ventilation in the OSC-greenhouse resulting in greater energy consumption during the day. This additional ventilation need is sporadic throughout the winter but is one contributing factor to the reduced energy load savings when going to a cold climate.

Now considering July, we find that it was more difficult to meet the temperature set-point for both the conventional and OSC-greenhouses in the warmer climates. As seen in Figure 5D the fan and pad cooling system is operating nearly the entire day in July in AZ. The inability to meet the temperature set-point is a common challenge in warm climates, and typical practice is to continue operations while cooling to the full possible extent. When moving to colder climates, both greenhouse types can improve their ability to meet the temperature set-points and the cooling loads are similar between conventional and OSC greenhouse systems. Here, it is important to note that in Figure 5 there is a discontinuity in the temperature and energy consumption data from 24 to 0 h. This is due the analysis using typical

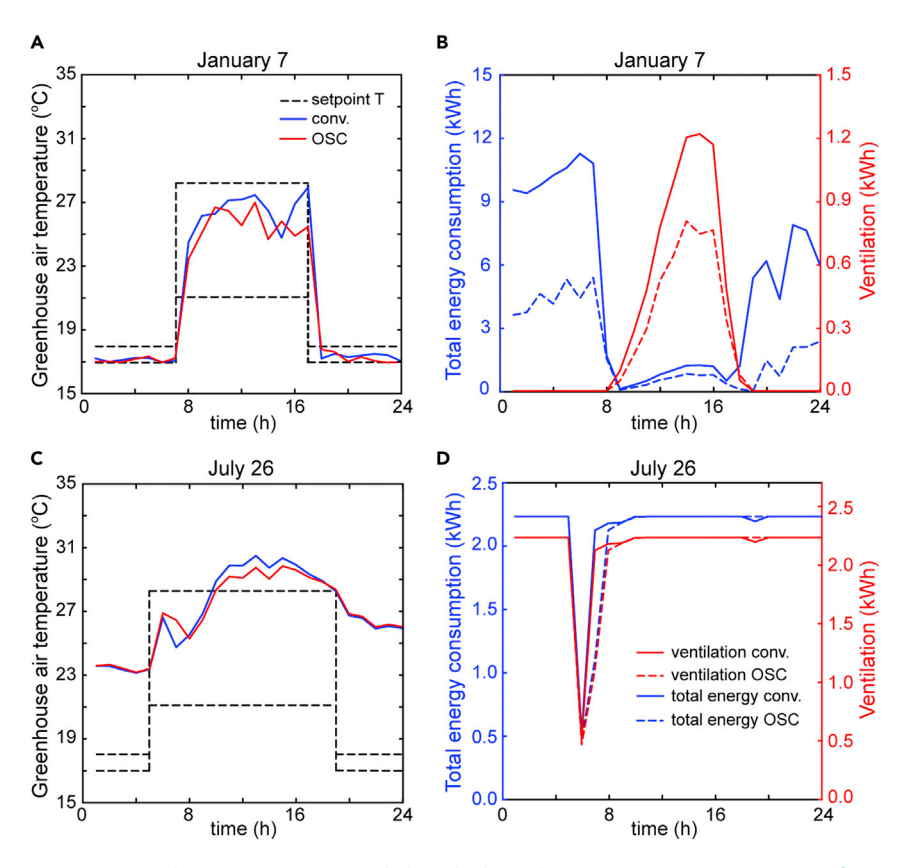


Figure 5. Greenhouse Air Temperature below Shades and Energy Consumption in Arizona for Conventional and PTB7-TH:IEICO-4F OSC Integrated Greenhouse

- (A) Air temperature for a typical day in January.
- (B) Electric energy consumption for fan and pad cooling and total energy consumption for a typical day in January.
- (C) Air temperature for a typical day in July.
- (D) Electric energy consumption for fan and pad cooling and total energy consumption for a typical day in July.

meteorological year data on an hourly basis. We select representative days of the season, but each day has a unique weather pattern and resulting in a unique greenhouse load.

Solar Cell Impact on Greenhouse Heating and Cooling Demand

The combination of the ITO electrodes and the 4-layer dielectric coating in the OSC stack increases the reflectance in the IR portion of the solar spectrum thereby lowering the thermal emissivity of the OSC-greenhouse with respect to the conventional greenhouse. The low-e nature of the OSCs reduce the radiation heat loss from inside the greenhouse lowering the heating demand as shown in Figures 3 and 5. The reduced heating is observed in all three locations considered. However, the heating load savings reduces as the greenhouse moves toward colder climates due in part to the reduced transmittance of the OSC stack lowering the solar heat gain during the day. In colder climates with higher heating loads, the loss of sunlight transmitted into the greenhouse results in a greater need for external thermal input for temperature and humidity control. Similar to the heating demand, the annual cooling load for the OSC-greenhouse reduces in comparison to a conventional greenhouse due to lower solar heat gain throughout the year. This reduced solar

CellPress

gain is from the high reflectivity of the OSC in the infrared region of the solar spectrum and the lower net transmittance of the OSC stack in comparison to the conventional greenhouse. The reduction in total radiation entering the OSC-greenhouse during the summer lowers the cooling load and removes the need for commonly employed shade cloths that are used in conventional greenhouses in the summer to avoid overheating. Hence, the OSCs employed provide better temperature control inside the OSC-greenhouse in comparison to the conventional greenhouse even if the greenhouse air temperature still frequently exceeds the set-point temperature during summer.

Achieving Net Zero Energy (NZE) Greenhouses

In all three selected locations (AZ, NC, and WI), the annual heating demand forms a significant fraction of the total energy demand. In AZ, NC and WI, the heating demand accounts for 50%, 75%, and 94% of the total energy demand respectively. Comparing the energy load in all the three locations, we find that Phoenix, AZ by virtue of its low heating demand and high solar insolation, provides ideal conditions for an OSC-greenhouse leading to a large annual surplus energy generation. In addition, the OSC-greenhouse does not observe a large drop in irradiance over PAR due in part to the large use of shade cloths in this climate. Hence, there is immense potential to achieve NZE greenhouses in Phoenix, AZ with minimal impact on plant growth. In both NC and WI, the solar cells continue to produce a surplus of energy in the summer but are unable to meet the monthly demand in portions of the winter months. On an annual basis, we find that in NC the solar cells exceed greenhouse energy demand thereby also providing potential for achieving NZE greenhouses. In WI, the cold climate incurs a significant heating load in the winter that the solar cells could not meet. However, applying additional energy conservation measures, higher efficiency solar cells, and modified operating schemes such as winter shut downs will improve the prospects of achieving a NZE greenhouse in cold climates.

Extrapolating Performance Using Conceptualized Organic Absorbers

So far, we considered high efficiency OSC active layers that partially absorb over the PAR spectrum. While this method succeeds in offsetting greenhouse energy demand, it may or may not be the best absorption characteristics for greenhouse integration without impacting plant growth. As a simple approximation to explore the opportunities associated with changing the absorption characteristics of the active layer, we consider a conceptual active organic semiconductor layer. We start by modelling the organic semiconductor absorption coefficient as a primary optical transition with two additional vibronic bands that are broadened using a Gaussian distribution function in energy. 65,66 The absorption coefficient was then converted to extinction coefficient. The magnitude of the extinction coefficient and bandwidth of absorption are chosen to match commonly observed values in organic semiconductors. 66 Additional common features in the absorption profile such as an extended tail at higher energies, and higher energy band transitions are not included due to the large variation in possible absorption profiles. 65 Once the extinction coefficient was estimated the refractive index was determined via Kramer-Kronig relations. Two of these conceptual materials were created to approximate the donor and acceptor of the active layer and set to have complimentary absorption bands resulting in an approximate 400 nm bandwidth, as shown in Figures 6 and \$10. The donor and acceptor material are assumed to be blended 1:1 by volume. The absorption edge of the active layer (which defines the semiconductor bandgap) was then freely defined. In this model, the solar cell had the same device architecture given in Figure 2A but without the 4-layer dielectric coating. For each bandgap considered, the thickness of the active layer was varied to ensure an



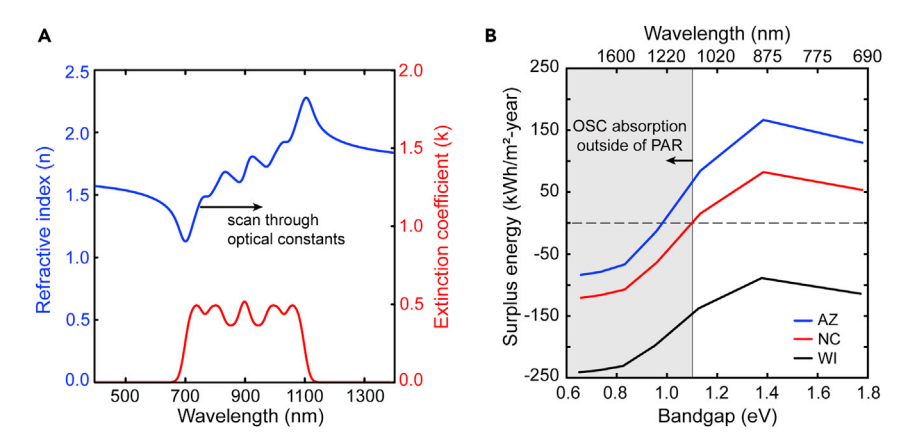


Figure 6. Modelling Conceptualized Organic Solar Cell

(A) Idealized optical constants for an organic solar cell absorbing with an absorption bandwidth of 400 nm and an absorption edge at 1,100 nm (or 1.13 eV).

(B) Surplus energy generation as a function of solar cell band gap (defined by the solar cell absorption edge) for a greenhouse in Arizona (AZ), North Carolina (NC), and Wisconsin (WI).

average transmittance over PAR of at least 35% which is comparable to the OSCs considered above. A maximum thickness of the active layer was set to 300 nm.

To determine the power generation of this OSC, we continue to use the same approach to estimate J_{SC} as described above, and the fill factor was set to 0.7. The V_{OC} of the solar cell under 1-sun illumination was taken as the bandgap energy (E_{α}) of the active layer divided by a unit charge (q) and included a 0.3 V loss ($E_{\rm q}/{\rm q}$ – 0.3 V). While OSCs with voltage losses less than 0.1 V have been demonstrated,⁶⁷ we choose a conservative 0.3 V loss similar to that observed in PTB7-TH:IEICO-4F OSCs.²⁵ The V_{OC} was then varied depending on the photocurrent using the same approach as the material defined active layers. Through this analysis we find that as the active layer absorption moves into the IR to limit overlap of absorption between the OSCs and plants (Figure 1D), there is a reduction in the ability of the solar cell to meet the energy needs of the greenhouse, as shown in Figure 6B. However, we find that the conceptualized solar cells with absorption predominately outside the PAR spectrum is still able to achieve an annual surplus in energy for an OSC-greenhouse in AZ, and meets the annual energy demand in NC. Thus, OSCs with minimal absorption overlap with PAR can achieve NZE greenhouses in warm and moderate climates. In WI, no bandgap value considered was able to meet the energy demand of the greenhouse. While this is a simple model, these results show that there is a rich opportunity to optimize organic solar cells to balance light absorption for power generation to meet the energy load of the greenhouse while also optimizing transmittance for plant growth.

Conclusions

Through a detailed custom-tailored dynamic energy balance model, we considered the opportunity for semitransparent organic solar cells to be integrated onto greenhouse structures to achieve NZE controlled environment agriculture. The analysis considered two solar cells active layers in 3 distinct climates. We find that in hot (AZ) and mixed-humid (NC) climates, that OSC-greenhouses could generate the energy necessary to manage the thermal load of the facility throughout the year. In AZ and NC there is a significant surplus in solar power generation suggesting opportunities to support supplemental lighting or feed electricity into the grid. However, this



model only considered static solar cells and limited design optimization and it is expected that further improvements are possible.

The analysis also revealed that there are significant energy load savings when integrating the OSCs solely due to the low-e nature of the ITO electrodes and optical coating. The low-e coating reduces IR transmittance from sunlight reducing overheating, and also increases IR reflectance from thermal radiation from within the greenhouse, thereby retaining the thermal energy inside the greenhouse during the night. Through the improved thermal trapping at night, the OSC-greenhouses have significantly lower energy demand in the winter in all three locations. The reduction in the heating load of the greenhouse with the OSC addition ranges from 54% in AZ, 46% in NC, and 32% in WI. Although, the OSC power generation in WI did not meet the greenhouse energy demand, the drop in heating demand constitutes a significant energy savings making the overall greenhouse production more attractive in cold climates. It was found that there was not a significant difference in the cooling demand between the conventional and OSC-greenhouses when compared to the savings in heating demand. This is associated with the addition of OSCs resulting in a similar sunlight transmittance reduction as the deployed shades in the conventional greenhouse. While the energy savings aren't as significant in the summer, the solar cells effectively act as the shade with the added benefit of harnessing the excess energy. A second important insight of this modelling is that the irradiance over the PAR waveband entering the OSC-greenhouse was not reduced as significantly as the OSC transmittance would suggest. There are two primary reasons for this including, a significant portion of sunlight entering through the uncoated walls of the greenhouse and the removal of the need for shade cloths during the summer. The use of OSCs as replacements for shadecloths is particularly beneficial in hot climates (AZ) where shade cloths are used over a larger portion of the year. The change in irradiation on plant growth was not considered explicitly and this is an important consideration for future study. As a first approximation, we considered changes in active layer thickness to balance power generation and radiation entering the greenhouse. We found that the energy needs of the greenhouse could be met in AZ and NC with an annual reduction in PAR radiation of only 10% in AZ and 25% in NC. The expected OSC-greenhouse performance if the active layer absorption characteristics could be modified to compliment the plant growth as needed was also considered. In the case of the active layer absorption being predominately outside of PAR, we find that the OSCs are able to meet the energy demand of greenhouses in AZ and in NC. In our analysis, a thorough optimization of the solar cell design, orientation, deployment strategy, as well as greenhouse operating practice was not completed. It is expected that further gains in system performance are likely possible with further optimization. Nevertheless, given realistic solar cell performance metrics and greenhouse energy demands, it is clearly found that the solar power generation can supply most if not all the energy needs of the greenhouse in warm and moderate climates.

Overall, our modeling demonstrates that there are significant opportunities for achieving net-zero energy OSC-greenhouse operation and provides a foundation for future optimization. With the developed energy model being able to predict energy load, solar power generation, and light entering the greenhouse, there is immense scope to utilize the data to explore options for energy storage, solar cell optimization, supplemental lighting, and plant growth optimization. The results also support further research into improved and stable semitransparent OSCs.



SUPPLEMENTAL INFORMATION

Supplemental Information can be found online at https://doi.org/10.1016/j.joule. 2019.12.018.

ACKNOWLEDGMENTS

The authors would like to acknowledge the National Science Foundation, United States, INFEWS award CBET-1639429 for support of this research.

AUTHOR CONTRIBUTIONS

B.O. directed the study. E.R. formulated the greenhouse energy model with contributions from B.O. B.O., H.A., and H.S. contributed to the conceptual framework of the study. C.S. and H.S. contributed to the greenhouse design, H.A. and B.O. contributed to the organic solar cell design and implementation. R.B. measured the optical constant for PTB7-TH:IEICO-4F. E.R. wrote the original draft, and all authors contributed to the analysis and the writing.

DECLARATION OF INTERESTS

The authors declare no competing interests

Received: August 27, 2019 Revised: November 12, 2019 Accepted: December 20, 2019 Published: January 29, 2020

REFERENCES

- Vos, R., Bellù, L.G., Stamoulis, K., and Haight, B. (2017). The Future of Food and Agriculture – Trends and Challenges (Food and Agriculture Organisation of the United Nations).
- Beddington, J., Asaduzzaman, J., Clark, M., Fernández, A., Guillou, M., Jahn, M., Erda, L., Mamo, T., Van Bo, N., Nobre, C.A., et al. (2012). Achieving Food Security in the Face of Climate Change: Final Report from the Commission on Sustainable Agriculture and Climate Change (CGIAR Research Program on Climate Change, Agriculture and Food Security).
- Cook, R., and Calvin, L. (2005). Greenhouse tomatoes change the dynamics of the North American fresh tomato industry, Economic Research Report No. 2 (USDA).
- Bot, G., Van De Braak, N., Challa, H., Hemming, S., Rieswijk, T., van Straten, G.V., and Verlodt, I. (2005). The solar greenhouse: state of the art in energy saving and sustainable energy supply. Acta Hortic. 691, 501–508.
- 5. Green, M.A. (2019). How did solar cells get so cheap? Joule *3*, 631–633.
- Lee, T.D., and Ebong, A.U. (2017). A review of thin film solar cell technologies and challenges. Renew. Sustain. Energy Rev. 70, 1286–1297.
- Brus, V.V., Lee, J., Luginbuhl, B.R., Ko, S.J., Bazan, G.C., and Nguyen, T.Q. (2019). Solution-processed semitransparent organic photovoltaics: From molecular design to device performance. Adv. Mater. 31, e1900904.
- 8. Hassanien, R.H.E., Li, M., and Dong Lin, W. (2016). Advanced applications of solar energy

- in agricultural greenhouses. Renew. Sustain. Energy Rev. *54*, 989–1001.
- Allardyce, C.S., Fankhauser, C., Zakeeruddin, S.M., Grätzel, M., and Dyson, P.J. (2017). The influence of greenhouse-integrated photovoltaics on crop production. Sol. Energy 155, 517–522.
- Hollingsworth, J.A., Ravishankar, E., O'Connor, B., Johnson, J.X., and DeCarolis, J.F. (2019). Environmental and economic impacts of solar powered integrated greenhouses. J. Ind. Ecol. 1, 14
- Cossu, M., Murgia, L., Ledda, L., Deligios, P.A., Sirigu, A., Chessa, F., and Pazzona, A. (2014).
 Solar radiation distribution inside a greenhouse with south-oriented photovoltaic roofs and effects on crop productivity. Appl. Energy 133, 89–100.
- Yano, A., Kadowaki, M., Furue, A., Tamaki, N., Tanaka, T., Hiraki, E., Kato, Y., Ishizu, F., and Noda, S. (2010). Shading and electrical features of a photovoltaic array mounted inside the roof of an east-west oriented greenhouse. Biosyst. Eng. 106, 367–377.
- Yano, A., Onoe, M., and Nakata, J. (2014). Prototype semi-transparent photovoltaic modules for greenhouse roof applications. Biosyst. Eng. 122, 62–73.
- Kadowaki, M., Yano, A., Ishizu, F., Tanaka, T., and Noda, S. (2012). Effects of greenhouse photovoltaic array shading on Welsh onion growth. Biosyst. Eng. 111, 290–297.
- Sonneveld, P.J., Swinkels, G.L.A.M., Campen, J., Van Tuijl, B.A.J., Janssen, H.J.J., and Bot,

- G.P.A. (2010). Performance results of a solar greenhouse combining electrical and thermal energy production. Biosyst. Eng. 106, 48–57.
- Corrado, C., Leow, S.W., Osborn, M., Chan, E., Balaban, B., and Carter, S.A. (2013).
 Optimization of gain and energy conversion efficiency using front-facing photovoltaic cell luminescent solar concentrator design. Sol. Energy Mater. Sol. Cells 111, 74–81.
- Emmott, C.J.M., Röhr, J.A., Campoy-Quiles, M., Kirchartz, T., Urbina, A., Ekins-Daukes, N.J., and Nelson, J. (2015). Organic photovoltaic greenhouses: a unique application for semitransparent PV? Energy Environ. Sci. 8, 1317– 1229.
- Sonneveld, P.J., Swinkels, G.L.A.M., Bot, G.P.A., and Flamand, G. (2010). Performance results of a solar greenhouse combining electrical and thermal energy production. Biosyst. Eng. 105, 51–58.
- Azzopardi, B., Emmott, C.J.M., Urbina, A., Krebs, F.C., Mutale, J., and Nelson, J. (2011). Economic assessment of solar electricity production from organic-based photovoltaic modules in a domestic environment. Energy Environ. Sci. 4, 3741–3753.
- Krebs, F.C., Espinosa, N., Hösel, M., Søndergaard, R.R., and Jørgensen, M. (2014).
 anniversary article: rise to power - OPV-based solar parks. Adv. Mater. 26, 29–38.
- Mulligan, C.J., Wilson, M., Bryant, G., Vaughan, B., Zhou, X., Belcher, W.J., and Dastoor, P.C. (2014). A projection of commercial-scale



- organic photovoltaic module costs. Sol. Energy Mater. Sol. Cells *120*, 9–17.
- Ashworth, C., Barlow, S., Wang, Z., Yan, H., Jen, A.K.Y., Marder, S.R., and Zhan, X. (2018). Interrogating the interphase. Nat. Rev. Mater. 3, 1–19.
- Cui, Y., Yao, H., Zhang, J., Zhang, T., Wang, Y., Hong, L., Xian, K., Xu, B., Zhang, S., Peng, J., et al. (2019). Over 16% efficiency organic photovoltaic cells enabled by a chlorinated acceptor with increased open-circuit voltages. Nat. Commun. 10, 2515.
- Zhao, J., Li, Y., Yang, G., Jiang, K., Lin, H., Ade, H., Ma, W., and Yan, H. (2016). Efficient organic solar cells processed from hydrocarbon solvents. Nat. Energy 1, 15027.
- Song, X., Gasparini, N., Ye, L., Yao, H., Hou, J., Ade, H., and Baran, D. (2018). Controlling blend morphology for ultrahigh current density in nonfullerene acceptor-based organic solar cells. ACS Energy Lett. 3, 669–676.
- Liu, Y., Cheng, P., Li, T., Wang, R., Li, Y., Chang, S.Y., Zhu, Y., Cheng, H.W., Wei, K.H., Zhan, X., et al. (2019). Unraveling sunlight by transparent organic semiconductors toward photovoltaic and photosynthesis. ACS Nano 13, 1071–1077.
- Corrado, C., Leow, S.W., Osborn, M., Carbone, I., Hellier, K., Short, M., Alers, G., and Carter, S.A. (2016). Power generation study of luminescent solar concentrator greenhouse. J. Renewable Sustainable Energy 8.
- Ye, L., Xiong, Y., Zhang, Q., Li, S., Wang, C., Jiang, Z., Hou, J., You, W., and Ade, H. (2018). Surpassing 10% efficiency benchmark for nonfullerene organic solar cells by scalable coating in air from single nonhalogenated solvent. Adv. Mater. 30.
- Baechler, M.C., Gilbride, T.L., Cole, P.C., Hefty, M.G., and Ruiz, K. (2015). Guide to Determining Climate Regions by County Vol. 7.3, Building America Best Practices Series (United States Department of Energy).
- Sethi, V.P., Sumathy, K., Lee, C., and Pal, D.S. (2013). Thermal modeling aspects of solar greenhouse microclimate control: a review on heating technologies. Sol. Energy 96, 56–82.
- Walker, J.N. (1965). Predicting temperatures in ventilated greenhouses. Trans. ASAE 8, 445–448.
- 32. Chandra, P., Albright, L.D., and Scott, N.R. (1981). Time dependent analysis of greenhouse thermal environment. Trans. ASAE 24, 442–449.
- 33. Tiwari, G.N. (1985). Analysis of winter greenhouse. Int. J. Sol. Energy 3, 19–24.
- 34. Kimball, B.A. (1973). Simulation of the energy balance of a greenhouse. Agric. Meteorol. 11, 243–260.
- Cooper, P.I., and Fuller, R.J. (1983). A transient model of the interaction between crop, environment and greenhouse structure for predicting crop yield and energy consumption. J. Agric. Eng. Res. 28, 401–417.
- **36.** Fabrizio, E. (2012). Energy reduction measures in agricultural greenhouses heating: envelope,

- systems and solar energy collection. Energy Build. 53, 57–63.
- 37. Avissar, R., and Mahrer, Y. (1982). Verification study of a numerical greenhouse. Trans. ASAE 25, 1711–1720.
- **38.** Wilcox, S., and Marion, W. (2008). User Manual for TMY3 Data Sets (NREL).
- 39. Jolliet, O. (1994). HORTITRANS, a model for predicting and optimizing humidity and transpiration in greenhouses. J. Agric. Eng. Res. 57, 23–37.
- Ahamed, M.S., Guo, H., and Tanino, K. (2018). A quasi-steady state model for predicting the heating requirements of conventional greenhouses in cold regions. Inf. Process. Agric. 5, 33–46.
- Semple, L., Carriveau, R., and Ting, D.S.K. (2017). Assessing heating and cooling demands of closed greenhouse systems in a cold climate. Int. J. Energy Res. 41, 1903–1913.
- 42. Fisher, P., and Runkle, E. (2004). Lighting up profits: understanding greenhouse lighting (Meister Media Wordwide).
- Schwarz, D., Thompson, A.J., and Kläring, H.P. (2014). Guidelines to use tomato in experiments with a controlled environment. Front. Plant Sci. 5, 625.
- 44. Heuvelink, E.P. (2018). Tomatoes (CAB International).
- Fitz-Rodríguez, E., Kubota, C., Giacomelli, G.A., Tignor, M.E., Wilson, S.B., and McMahon, M. (2010). Dynamic modeling and simulation of greenhouse environments under several scenarios: A web-based application. Comput. Electron. Agric. 70, 105–116.
- Owen, M.S. (2015). ASHRAE Handbook HVAC Applications (ASHRAE).
- Al-Ibrahim, A., Al-Abbadi, N., and Al-Helal, I. (2006). PV greenhouse system - System description, performance and lesson learned. Acta Hortic. 710, 251–264.
- Al-Helal, I.M. (2007). Effects of ventilation rate on the environment. Appl. Eng. Agric. 23, 221–230.
- Chandra, P., and Albright, L.D. (1980).
 Analytical determination of the effect on greenhouse heating requirements of using night curtains. Trans. ASAE 23, 994–1000.
- Gent, M.P.N. (2007). Effect of shade on quality of greenhouse tomato. Hortscience 42, 514–520.
- Kempkes, F.L.K., and Hemming, S. (2012). Calculation of NIR effect on greenhouse climate in various conditions. Acta Hortic. 927, 543–550.
- McCree, K.J. (1971). The action spectrum, absorptance and quantum yield of photosynthesis in crop plants. Agric. Meteorol. 9, 191–216.
- Gueymard, C. (2000). Prediction and performance assessment of mean hourly global radiation. Sol. Energy 68, 285–303.

- 54. Goswami, D.Y. (2015). Principles of Solar Engineering (CRC Press).
- Wojcicki, D.J. (2015). Derivation of the effective beam radiation incidence angle equations for diffuse and reflected solar radiation using a two dimensional approach. Sol. Energy 112, 272–281.
- Stackhouse, P.W., Chandler, W.S., Whitlock, C.H., Hoell, J.M., Westberg, D., and Zhang, T. (2007). NASA's surface meteorology and solar energy web portal (Release 6.0). Proceedings of the Solar Conference 1, 17–22.
- Centurioni, E. (2005). Generalized matrix method for calculation of internal light energy flux in mixed coherent and incoherent multilayers. Appl. Opt. 44, 7532–7539.
- Pettersson, L.A.A., Roman, L.S., and Inganäs, O. (1999). Modeling photocurrent action spectra of photovoltaic devices based on organic thin films. J. Appl. Phys. 86, 487–496.
- Shi, H., Xia, R., Zhang, G., Yip, H.L., and Cao, Y. (2019). Polymer solar cells: spectral engineering of semitransparent polymer solar cells for greenhouse applications. Adv. Energy Mater. 9.
- Dyer-Smith, C., Nelson, J., and Li, Y. (2018). McEvoy's Handbook of Photovoltaics (Academic Press).
- Alonso-Álvarez, D., Ferre Llin, L., Mellor, A., Paul, D.J., and Ekins-Daukes, N.J. (2017). ITO and AZO films for low emissivity coatings in hybrid photovoltaic-thermal applications. Sol. Energy 155, 82–92.
- Sun, C., Xia, R., Shi, H., Yao, H., Liu, X., Hou, J., Huang, F., Yip, H., and Cao, Y. (2018). Heatinsulating multifunctional semitransparent polymer solar cells. Joule 2, 1816–1826.
- 63. Kitchen, B., Awartani, O., Kline, R.J., McAfee, T., Ade, H., and O'Connor, B.T. (2015). Tuning open-circuit voltage in organic solar cells with molecular orientation. ACS Appl. Mater. Interfaces 7, 13208–13216.
- Reichelstein, S., and Yorston, M. (2013). The prospects for cost competitive solar PV power. Energy Policy 55, 117–127.
- Krückemeier, L., Kaienburg, P., Flohre, J., Bittkau, K., Zonno, I., Krogmeier, B., and Kirchartz, T. (2018). Developing design criteria for organic solar cells using well-absorbing non-fullerene acceptors. Commun. Phys. 1, 27.
- Vezie, M.S., Few, S., Meager, I., Pieridou, G., Dörling, B., Ashraf, R.S., Goñi, A.R., Bronstein, H., McCulloch, I., Hayes, S.C., et al. (2016). Exploring the origin of high optical absorption in conjugated polymers. Nat. Mater. 15, 746–753.
- 67. Ullbrich, S., Benduhn, J., Jia, X., Nikolis, V.C., Tvingstedt, K., Piersimoni, F., Roland, S., Liu, Y., Wu, J., Fischer, A., et al. (2019). Emissive and charge-generating donor-acceptor interfaces for organic optoelectronics with low voltage losses. Nat. Mater. 18, 459–464.